ACS MEASUREMENT SCIENCE Au
AN OPEN ACCESS JOURNAL OF THE AMERICAN CHEMICAL SOCIETY

pubs.acs.org/measureau
Article

3D Paper-Based Device Integrated with a Battery-Less NFC Potentiostat for Nonenzymatic Detection of Cholesterol

Published as part of ACS Measurement Science Au virtual special issue "2024 Rising Stars".

Sudkate Chaiyo,* Kanjana Kunpatee, Kurt Kalcher, Abdulhadee Yakoh, and Kingkan Pungjunun

Cite This: *ACS Meas. Sci. Au* 2024, 4, 432−441
Read Online

ACCESS | Metrics & More | Article Recommendations | Supporting Information

ABSTRACT: Portable electrochemical analytical devices such as cholesterol sensors are widely used for disease diagnosis. However, these tools are bulky and require bioreceptors for the specific detection of cholesterol. Herein, a novel 3D electrochemical paper-based analytical device (3D-ePAD) combined with a near-field communication (NFC) potentiostat was developed and applied to the nonenzymatic detection of cholesterol. This 3D-ePAD platform was designed so that all working operations are performed on a single device, which is separated into an origami PAD (oPAD) and an inset PAD (iPAD). β-Cyclodextrin (β-CD), which is immobilized on oPAD, is used as a specific material for the nonenzymatic detection of cholesterol. Through this device, cholesterol detection is integrated with a battery-free NFC potentiostat on a smartphone. The concentration of cholesterol was examined through a $[Fe(CN)_6]^{3-/4-}$ current signal as a redox indicator, which was previously stored in the detection part of an iPAD. Under optimal conditions, 3D-ePAD/NFC exhibited a linear detection efficiency of 1−500 μM and a maximum detection limit of 0.3 μM for cholesterol detection. Moreover, the proposed sensor was successfully used to measure cholesterol in real serum samples from humans, and the results were consistent with those of a commercial cholesterol meter. Therefore, the new NFC-operated 3D-ePAD platform can be used as an alternative tool for the nonenzymatic quantification of various biomarkers. In addition, 3D-ePAD/NFC can support the diagnosis of other diseases in the future, as the device is inexpensive, portable, and disposable and functions with low sample volumes.

KEYWORDS: *3D paper-based analytical device, Electrochemical detection, Near-field communication, Cholesterol, Nonenzymatic system*

1. INTRODUCTION

Coronary heart disease (CHD) or coronary artery disease significantly causes one-third of all mortalities worldwide.[1,2] CHD develops when the wall of the coronary artery has been filled by the buildup of fatty acids, especially fat-like substances created by the liver or consumed through animal products.[3] For clinical diagnosis, cholesterol levels in human serum can be measured to predict future CHD. The average cholesterol level in human serum is between 200 and 240 mg/dL.[4,5] Elevated cholesterol levels above 240 mg/dL indicate a risk of CHD,[5] hypertension,[6] Alzheimer's disease,[7] Parkinson's disease,[8] etc. Therefore, analytical methods with high sensitivity and selectivity are needed to measure cholesterol levels.

To date, the conventional methods for detecting the relative levels of cholesterol in a sample involve electrochemical biosensors that utilize an enzymatic reaction between cholesterol and cholesterol oxidase.[9] Consequently, the sensors exhibit good selectivity and are highly sensitive.[10] However, enzyme-based sensors are traditionally associated with high costs and inadequate long-term stability due to the denaturing of the protein in enzymes. Nonenzymatic cholesterol biosensors have rapidly gained significant attention and have been developed to improve the limitations of enzyme assays and achieve sensors with a long shelf life, low cost, and simplicity.[11−13] Nonenzymatic sensing is operated through the catalytic activity of the catalyst's direct cholesterol redox reaction; however, the sensors are limited by their poor selectivity with the common electroactive species in the actual sample, such as ascorbic acid and uric acid.[14]

β-Cyclodextrin (β-CD), a cyclic oligosaccharide, is characterized by a hydrophilic periphery face and a hydrophobic interior cavity. Therefore, the molecular recognition of β-CD is generally based on the host−guest interaction mechanism

Received: March 11, 2024
Revised: March 28, 2024
Accepted: April 8, 2024
Published: April 15, 2024

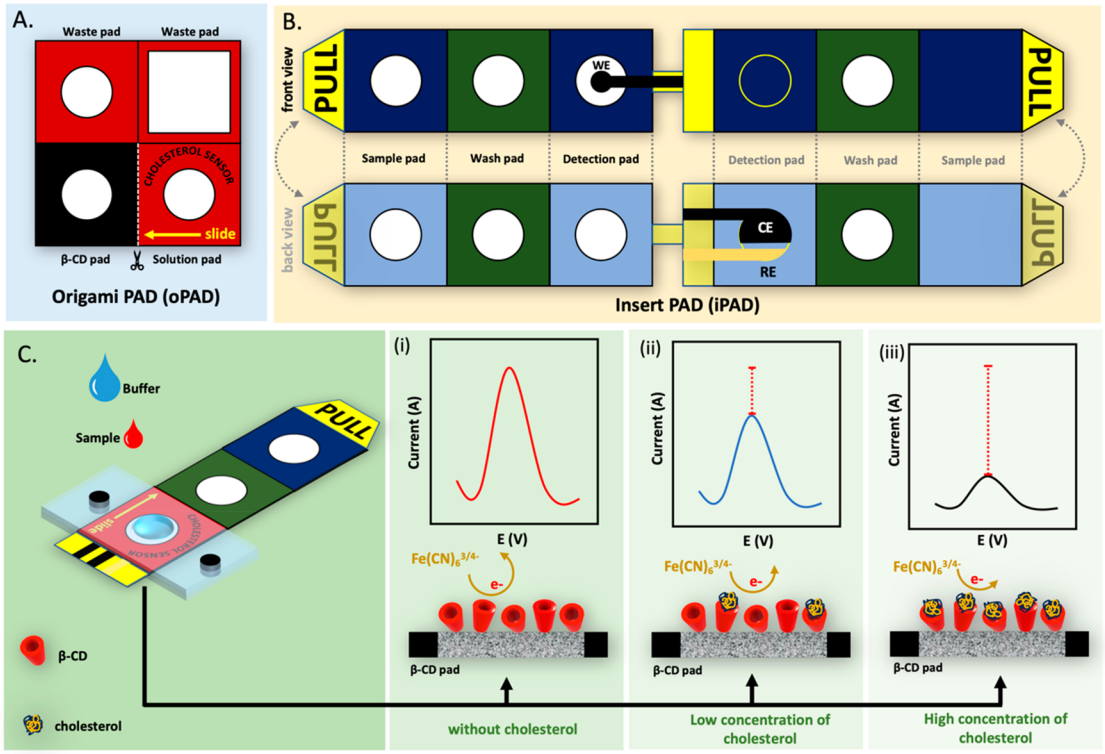

Figure 1. Design and composition of the 3D-ePAD includes (A) origami PAD (oPAD) and (B) inset PAD (iPAD), (C) diagram showing the concept of cholesterol detection in (i) the absence of cholesterol and in the presence of (ii) low and (iii) high cholesterol concentrations.

between guests and the host of β-CD. As a small hydrophobic molecule, β-CD has been widely used to detect small molecules, especially cholesterol, due to its highly selective binding size and easy preparation.[15−17] Yang et al. developed a β-CD/poly(*N*-acetylcholine)/Gra-modified electrode and methylene blue (MB) as a redox indicator for highly selective cholesterol detection.[17] From the previous study,[17] the host−guest interaction between β-CD and cholesterol involves various factors such as hydrophobic interaction, hydrogen bonding, and electrostatic interactions. The strong hydrophobic interactions were occurred by inserting the cholesterol molecule into hydrophobic cavities of β-CD molecules. The hydrogen bonding occurs when the hydroxy group in the cyclohexanol portion of the cholesterol molecule forms a bond with the hydroxyl group of β-CD. For the electrostatic interactions, the negative charge on the surface of cholesterol can interact with the positive charge on β-CDs. Nonetheless, this proposed platform, which involves multiple steps for sample preparation and a washing step, has a major problem, i.e., the platform is not ready to use and is unsuitable for clinical diagnostic applications. Therefore, obtaining a ready-to-use biomarker sensor for clinical diagnosis has been a significant challenge in recent years.

To overcome these challenges, we introduce a 3D electrochemical paper-based analytical device (3D-ePAD) for the first time to detect cholesterol nonenzymatically using β-cyclodextrin (β-CD)-modified cellulose filter paper. Paper-based analytical devices (PADs) are among the most promising substrate materials utilized in this work due to their advantages, including low cost, simplicity, and portability.[18,19] In particular, paper, which is a biodegradable and combustible material, could be safely discarded after use to prevent infectiousness from being in contact with assays. Moreover, PADs could be designed to generate high flexibility and simplicity for even complicated analytical protocols (such as point-of-care diagnostic assays). However, 3D-ePAD requires medium to large potentiometers to detect electrochemical signals and may not be suitable for on-site applications. Near-field communication (NFC) potentiostats provide an alternative to potentiometers, are the size of an ATM card, and do not require batteries. The device is a wireless communication technology that creates a contactless connection between two compatible devices.[20−22] NFC readers are currently being used in various biosensor applications, such as medical diagnostics[23] and food safety monitoring.[24] Therefore, in this work, we combined NFC with paper devices for the first time to detect cholesterol.

Herein, 3D-ePAD was designed to integrate multiple steps for the detection of cholesterol using β-cyclodextrin (β-CD)-modified cellulose filter paper within a single device. In this platform, reagents can be stored in an inset PAD (iPAD) and transported sequentially to the origami PAD (oPAD) detection zone. The presence of cholesterol was determined through the electrochemical signal response of the redox indicator $[Fe(CN)_6]^{3-/4-}$, as shown in Figure 1C. This signal was tracked by an NFC reader combined with a smartphone. In particular, to demonstrate the potential effectiveness for practical use, we also applied the developed electrochemical biosensing in real human serum samples, and the results were compared with a commercial cholesterol instrument. Finally, this developed device is potentially inexpensive, portable, disposable, highly selective, and highly sensitive.

https://doi.org/10.1021/acsmeasuresciau.4c00012
ACS Meas. Sci. Au 2024, 4, 432−441

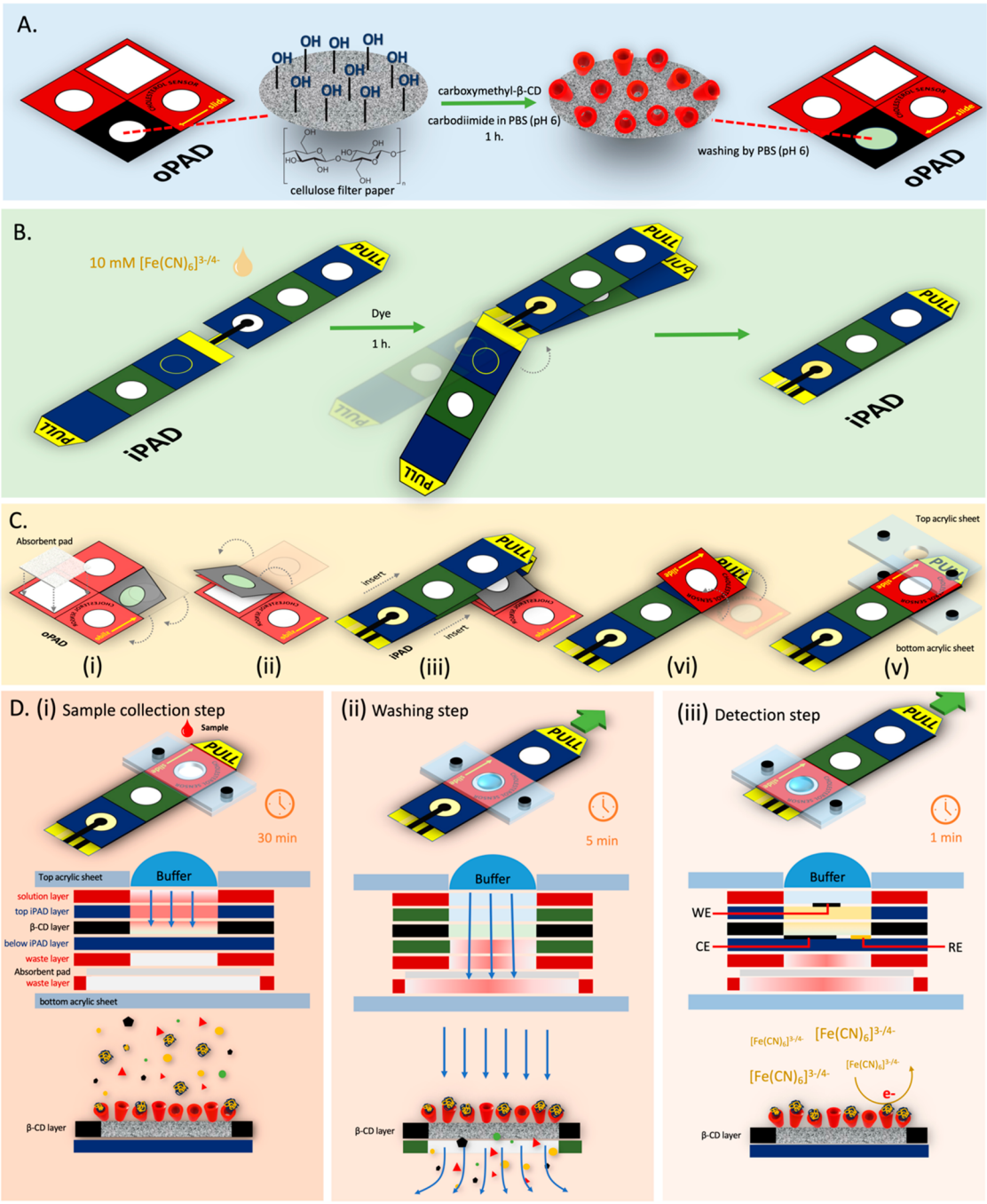

Figure 2. Illustration of preparation of (A) oPAD, (B) iPAD, and (C) 3D-ePAD. The 3D-ePAD operation (D) for cholesterol detection consists of sample loading (i), washing (ii), and detection steps(iii).

2. EXPERIMENTAL SECTION

2.1. Materials, Reagents, and Equipment

Details of the materials, equipment, and chemicals are presented in Supporting Information (SI).

2.2. Fabrication of 3D-ePAD

The 3D-ePAD comprises the following distinct components: an origami PAD (oPAD) utilized for *β*-CD-modified cellulose filter paper and an inset PAD (iPAD) designed for conducting multiple-step cholesterol detection, as shown in Figure 1. This device was meticulously designed using the Adobe Illustrator program, and details of the dimensions are shown in Figure S1. To establish a hydrophobic barrier, we implemented a wax-printing method was implemented. During the process of fabricating the device, the designated pattern was printed onto filter paper (specifically, Whatman No. 1) and subsequently subjected to an oven at a temperature of 150 °C for 60 s, allowing the wax to permeate through the paper. The oPAD (Figure 1A) was divided into three primary sections, namely, the *β*-CD-modified paper zone, the zone for introducing the sample and running buffer, and the waste reservoir (insert absorbent pad), which can be visualized in detail in Figure 1A.

Moreover, the iPAD comprises two distinct parts, denoted as Parts A and B, exhibiting mirror symmetry. Each of these components consists of three crucial elements, specifically the sampling zone, the washing zone, and the detection zone, all of which have been illustrated meticulously in Figure 1B. Importantly, a graphene conductive ink screen is printed on the front side of the detection zone (Part A), serving as the working electrode. In contrast, the counter electrode and reference electrode are represented by

https://doi.org/10.1021/acsmeasuresciau.4c00012
ACS Meas. Sci. Au 2024, 4, 432−441

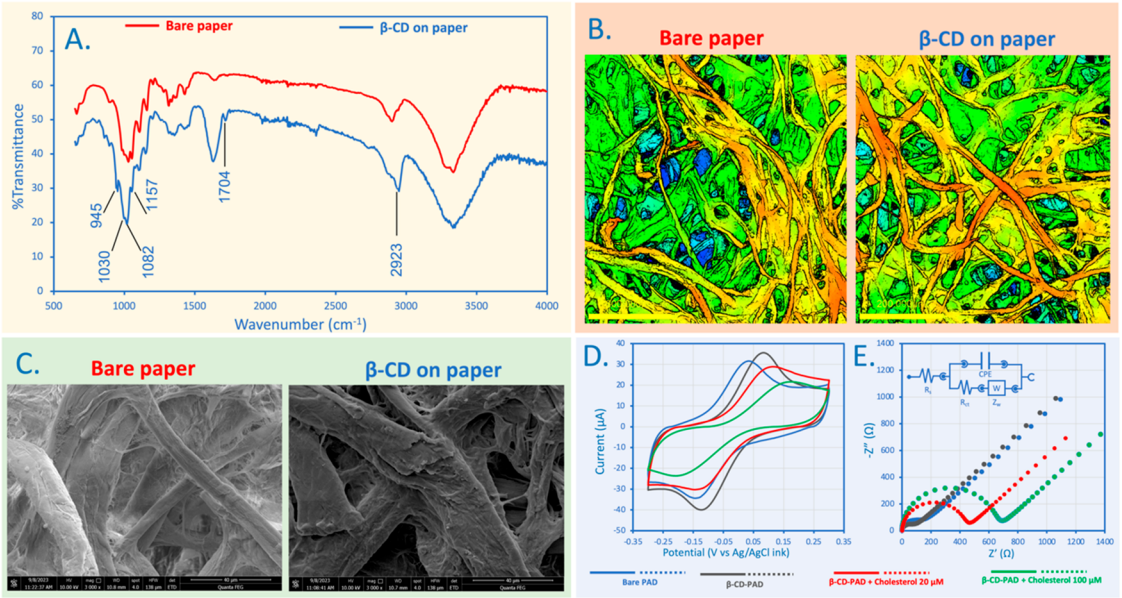

Figure 3. FTIR spectra of bare paper and β-CD-modified PAD (A), images of (left) bare paper and (right) β-CD-modified PAD using (B) confocal microscopy and (C) scanning electron microscopy (SEM), and the electrochemical behavior of each operation step using (D) CV and (E) EIS technique in 0.1 M KCl solution containing 10 mM $[Fe(CN)_6]^{3-/4-}$. The CV technique was performed with potential scanning from −0.3 to 0.3 V vs Ag/AgCl at a scan rate of 0.1 V/s. The EIS analysis was conducted with a 0.1 V AC potential over a frequency range from 0.1 to 100,000 Hz.

graphene conductive ink and Ag/AgCl ink, respectively, both of which were screen-printed on the backside of the detection zone (Part B). Following this step, the iPAD was subjected to a drying process within the confines of the oven, which was set at 55 °C for 1 h. Subsequently, 10 μL of 10 mM $[Fe(CN)_6]^{3-/4-}$ was dyed at room temperature for 1 h as the mediator (Figure 2B), which was expertly applied to the detection zone, facilitating the current response within the label-free system.

2.3. Modification of β-Cyclodextrin on oPAD

According to a method previously described in the literature by Furusaki et al.,[25] the preparation of β-CD involved an initial treatment of 100 g of β-CD with 93 g of NaOH in a 16.3% v/v solution of chloroacetic acid (270 mL), followed by sonication for 30 min. Subsequently, carboxymethyl-β-CD was precipitated with methanol and dried at 40 °C under ambient conditions. To create β-cyclodextrin on oPAD, a 25 mg/mL solution of carbodiimide, which contained 3 mM phosphate-buffered saline (PBS) at a pH of 6, was added to functionalize 10 mg/mL of carboxymethyl-β-CD. This mixture was then sonicated for a total reaction time of 90 min. The functionalized carboxymethyl-β-CD was subsequently applied to the oPAD and incubated for 1 h; thus, the substance was covalently immobilized onto the PAD surface after the carboxymethyl-β-CD substituent was substituted with the hydroxy group (−OH) of cellulose. After the reaction was complete, the modified paper surface was washed using PBS at a pH of 6 (Figure 2A).

2.4. 3D-ePAD Operation

The 3D-ePAD was developed to integrate three key stages in the detection of cholesterol using β-CD modified on a PAD (β-CD-PAD) into a single device. These stages include sample collection, washing, and analysis. The 3D-ePAD comprises the following components: the oPAD, which is responsible for the β-CD modification on the PAD, and the iPAD, which facilitates the execution of multiple steps within the device. To assemble the device, the folded oPAD is inserted onto the rear section of the iPAD, as depicted in Figure 2C(i–iii). Subsequently, the sample inlet zone on the oPAD is folded onto the iPAD, forming the first layer (Figure 2C(vi)). The final constructed 3D-ePAD is presented in Figure 2C(v). At this point, the device is ready for utilization.

To facilitate the movement of the iPAD component in the developed device, 3D-ePAD was covered with punched acrylic sheets. This conurbation can be observed in Figure 2D. In the first step, the sample (50 μL) was introduced into the inlet zone. Subsequently, the sample flowed through the β-CD-PAD layer and underwent a 30 min incubation at room temperature. This incubation led to the immobilization of the target analyte within the cavity of the β-CD-PAD, as depicted in Figure 2D(i). Once the reaction was complete, the iPAD was slid upward, positioning the washing zone beneath and in alignment with the β-CD-PAD layer of the oPAD, as shown in Figure 2D(ii). To remove any unbound cholesterol, running buffer consisting of 3 mM PBS at pH 6 (500 μL) was applied for 5 min. After the washing step was complete, the iPAD was once again slid upward. At this stage, the three-electrode system was situated between the target analyte immobilized on the β-CD-PAD layer and the remaining buffer solution. The current response was subsequently measured by using the differential pulse voltammetry (DPV) technique, as illustrated in Figure 2D(iii). The working operation of the 3D-ePAD is displayed in the attached VDOS1 in SI.

2.5. Electrochemical Detection

To achieve electrochemical detection, a voltammetric experiment was conducted using the PGSTAT 128 N AutoLab potentiostat (manufactured by Metrohm, Switzerland) under the control of the corresponding software (Nova 2.0) and the SIC4341 potentiostat sensor interface chip with NFC type 2 (Silicon Craft Technology PLC., Thailand) under the control of Chemister Application. After the samples were collected and washed, differential pulse voltammetry (DPV) was employed, and a potential scan ranging from −0.15 to 0.50 V vs Ag/AgCl ink was utilized with an amplitude of 70 mV, a potential step of 10 mV, and an equilibrium time of 3 s for the AutoLab potentiostat; for the NFC potentiostat sensor on the smartphone, potential begin of −0.3 V, potential final of 0.6 V potential amplitude of 70 mV, pulse duration of 100 ms, potential step of 10 mV, time step of 500 ms, and scan rate of 0.1 V/s were utilized. For characterization, cyclic voltammetry (CV) and electrochemical impedance spectroscopy (EIS) were carried out. CV involved scanning from −0.3 to 0.3 V vs Ag/AgCl at a scan rate of 0.1 V/s. EIS was performed by applying an AC potential of 0.1 V across a frequency range spanning from 0.1 to 100,000 Hz.

2.6. Sample Preparation

All of the serum samples were directly subjected to analysis using 3D-ePAD without any preliminary treatment steps. To evaluate the

https://doi.org/10.1021/acsmeasuresciau.4c00012
ACS Meas. Sci. Au 2024, 4, 432−441

reliability and applicability of the proposed sensing method, these samples were also validated in parallel with the use of a commercial cholesterol meter called The EasyTouch GCHb.

3. RESULTS AND DISCUSSION

3.1. Characterization of β-CD on oPADs

First, functionalized carboxymethyl-β-CD modified on oPAD was synthesized through a carbodiimide method consisting of the following steps: (i) formation of a carboxyl group on β-CD using the reaction between chloroacetic acid and β-CD under alkaline conditions and (ii) covalently bonding carboxymethyl-β-CD onto cellulose on the PAD surface via carbodiimide activation. To confirm that β-CD was completely synthesized on PAD, Fourier transform infrared (FTIR) spectroscopy was performed in a wavenumber range of 400−4000 cm^{-1}. A comparison of FTIR spectra results between bare paper and β-CD-modified PAD is presented in Figure 3A (red line) and 3A (blue line), respectively. The four characteristic stretching vibration bands of β-CD appear at 945, 1030, 1157, and 1704 cm^{-1}.[25,26] First, the absorption peak at 945 cm^{-1} is assigned to the R-1,4-bond skeleton vibration of β-CD. In addition, the two characteristic absorption bands at 1030 and 1157 cm^{-1} correspond to the O−H bending and antisymmetric glycosidic (C−O−C) stretching vibrations, respectively. In particular, the successfully functionalized carboxymethyl on β-CD in this work was confirmed from the peak spectra results of the C═O stretching vibration at 1704 cm^{-1}. The peak is slightly different from the bare paper due to the formation of various carbonyl-containing linkages between the cyclodextrin and filter paper.[27] A similar observation was made by Joseph, Vincent et al. when they modified the bare paper with β-CD.[28] Therefore, these results indicate that carboxymethyl-β-CD was grafted onto the surface of cellulose on the PAD surface as β-CD-PAD.

In addition, the roughness and shape of 3D-ePAD were evaluated to validate the successful modification of β-CD on paper by using confocal microscopy and scanning electron microscopy (SEM). Figure 3B presents a comparison of the confocal photographs, with the left side depicting the bare PAD (left) and the right side illustrating the modification of β-CD on paper (right). Figure 3B distinctly indicates that β-CD on the paper displays diminished roughness, which was substantiated by measuring the roughness area (Ra)[29−31] of β-CD on the paper (Ra = 9.97); the value obtained was lower than that of the bare paper (Ra = 14.18). The reduction in the roughness of carbon paper by β-CD may be attributed to the occurrence of cross-linking events, involving covalent bonding, between carboxymethyl-β-CD and cellulose paper. The SEM image (Figure 3C) is congruous with the confocal photographs; compared to the SEM image of the bare PAD (left), the SEM image of β-CD on the paper (right) contains small scattered particles. As a result, it can be deduced that β-CD can be modified on PADs.

3.2. Electrochemical Characterization of 3D-ePADs

The process of constructing 3D-ePAD was characterized using cyclic voltammetry (CV) and electrochemical impedance spectroscopy (EIS) experiments. Figure 3D shows the CV of different electrode modifications in 10 mM $[Fe(CN)_6]^{3-/4-}$ as a redox probe prepared on iPAD. On the bare paper, a pair of well-defined redox peaks with a peak-to-peak separation (ΔEp) of 0.16 V was observed (blue line), indicating that the electron transfer rate at the interface on this device was normal. On β-CD-PAD, the redox peak currents of $[Fe(CN)_6]^{3-/4-}$ increased (black line), suggesting the presence of modified β-CD on the PAD, which would accelerate the electron transfer of ferricyanide. Finally, the current response markedly decreased, while the peak-to-peak separation (ΔEp = 0.23 V) increased when β-CD-PAD was incubated with cholesterol (red and green line). This decrease in current and increases in ΔEp correspond to an increase in cholesterol concentration. This phenomenon was observed due to interaction between β-CD and cholesterol, which hinders the redox probe's electron transfer on the electrode surface.

Furthermore, an EIS plot was obtained to confirm that surface immobilization occurs through surface charge transfer resistance (Rct; Figure 3E and Table S1). The Rct decreased after the bare paper (blue line) electrode was modified with β-CD (black line), as confirmed by the lower resistance observed in the CV results.[32,33] In contrast, the Rct values of the β-CD-PAD/cholesterol electrodes increased due to the higher surface resistance (red and green lines), indicating the success of immobilization of β-CD- and interaction of β-CD-cholesterol. Thus, the consistency between the results obtained from CV and EIS confirms that the 3D-ePAD device was successfully constructed.

3.3. Cholesterol Detection Using 3D-ePAD

The electrochemical measurement of cholesterol was performed utilizing the electrochemical response of the redox $[Fe(CN)_6]^{3-/4-}$ as an indicator through the DPV technique, in which the electrochemical signals are measured from traditional benchtop potentiostat instrumentation (PGSTAT 128 N AutoLab potentiostat) and an NFC potentiostat sensor (S341 potentiostat sensor). Herein, β-CD was covalently bonded onto the PAD surface as a cholesterol recognition substance in the proposed system. To evaluate the electrochemical characteristics of β-CD-PAD on SPE by a commercial potentiostat, DPV was performed by using 10 mM $[Fe(CN)_6]^{3-/4-}$ contained in the electrochemical detection zone in the presence and absence of cholesterol. The differential pulse voltammograms (DPVs) showed that the current signal of $[Fe(CN)_6]^{3-/4-}$ without target analyte appeared as a well-defined peak at 0.15 V vs Ag/AgCl on the β-CD-PAD (Figure 4A: black line) higher than the bare PAD (Figure 4A: blue line) using SPE. These phenomena clearly demonstrated that the electrochemical performance was more improved with β-CD-PAD combined with SPE because of its electrocatalysis than with the bare PAD. The observed increase in peak current can be ascribed to the supramolecular structures of β-CD, which facilitate easier access of the $[Fe(CN)_6]^{3-/4-}$ redox species to the electrode, as has been previously reported.[34−36] To obtain evidence of the proposed concept, 20 (red line) and 100 μM (green line) cholesterol were individually immobilized on β-CD-PAD for 30 min and subsequently tested using $[Fe(CN)_6]^{3-/4-}$ as a redox indicator on SPE. As clearly shown in Figure 4A, the current signal of $[Fe(CN)_6]^{3-/4-}$ significantly dropped with increasing cholesterol concentration; as a result, the nonconductive complex between β-CD and cholesterol (β-CD-cholesterol) hindered electron transfer on the electrode surface. Hence, in this work, β-CD-PAD combined with SPE was used as an effective system for the nonenzyme electrochemical detection of cholesterol using $[Fe(CN)_6]^{3-/4-}$ as a redox indicator. When this device was tested by an NFC potentiostat, as shown in Figure 4B, a peak was observed at 0.15 V, and this response was in the same direction as that of commercial instruments. Therefore, this research applied an

https://doi.org/10.1021/acsmeasuresciau.4c00012
ACS Meas. Sci. Au 2024, 4, 432−441

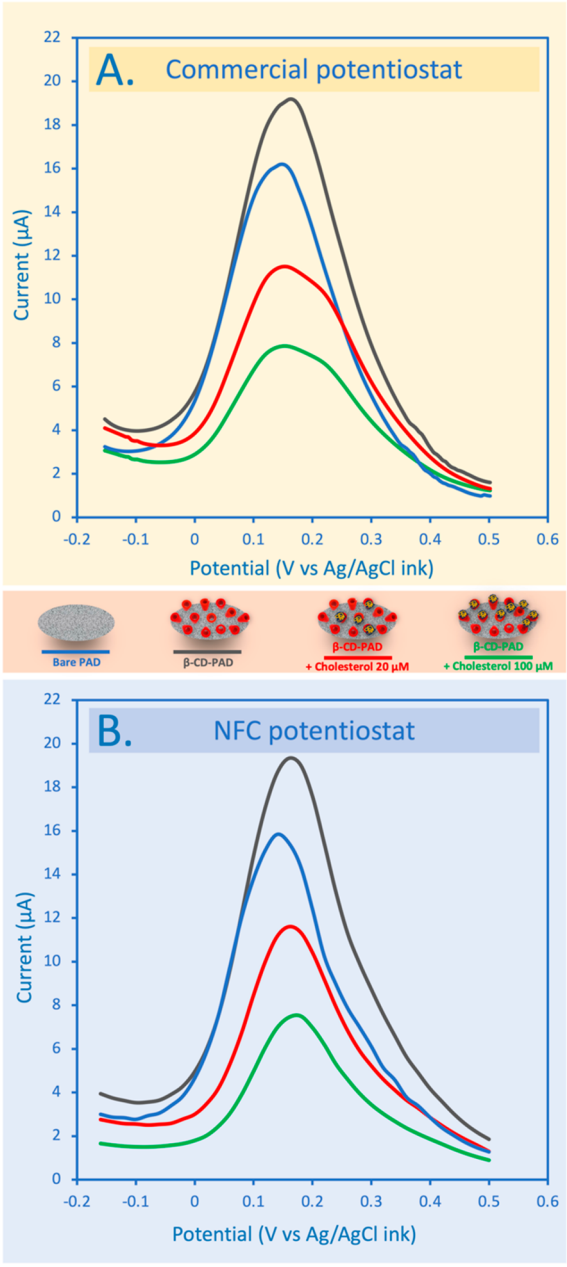

Figure 4. DPV responses of bare PAD, β-CD/PAD, 20 μM Cholesterol/β-CD/PAD, and 100 μM Cholesterol/β-CD/PAD using (A) the commercial potentiostat and (B) the NFC potentiostat.

NFC potentiostat with this device for cholesterol detection. Moreover, the current difference between the target analyte and buffer solution ($\Delta I = I_{\text{cholesterol}} - I_{\text{blank}}$) was used to quantify cholesterol in the following experiment.

3.4. Effect of β-CD Concentrations and Incubation Time

β-CD modified on PAD plays an essential role by improving the sensitivity and selectivity for the quantification of cholesterol. The recognition and capability of β-CD could exhibit high specificity with cholesterol through the selective binding size between an interior cavity and target molecule, which is known as the size/shape-fit concept. Thus, how the β-CD concentration affects the detection of 0.50 mM cholesterol was first studied over a range between 10 and 200 μg/mL after incubation for 30 min. As clearly shown in Figure S2A, the current difference response gradually decreased with increasing β-CD concentration and remained steady at 100 μg/mL. This result could indicate that PAD contained a limited amount of cholesterol-binding β-CD; therefore, the current difference was stable at the oversaturation point. Beyond 150 μg/mL β-CD, the current change slightly decreased as a result of the β-CD hidden electron transfer on the electrode surface. Consequently, 100 μg/mL β-CD was chosen as a modified condition on PAD for the selective detection of cholesterol. Afterward, the incubation time was subsequently investigated. As shown in Figure S2B, the highest current difference was achieved at 30 min and remained stable after this time. Therefore, an incubation time of 30 min was used for further experiments.

3.5. Analytical Performance of the Proposed Cholesterol Biosensor

As a proof of concept, the analytical performance of the proposed 3D-ePAD for the quantification of cholesterol under optimal conditions was evaluated by using a commercial potentiostat and NFC potentiostat, as shown in Figure S3 and Figure 5, respectively. The current response gradually decreased with increasing concentrations of cholesterol. As a result of the commercial potentiostat, the calibration plot presented an excellent linear logarithmic relationship between the current change (ΔI) and the concentration of cholesterol over a range from 0.1 to 1000 μM with the regression equation ΔI (μM) = 2.1233 log $C_{\text{cholesterol}}$ + 3.692 (R^2 = 0.9901), as shown in Figure S3. The limit of detection (LOD) (3SD/Slope) and quantification (LOQ) (10SD/Slope) were as low as 0.03 μM (30 nM) and 0.1 μM, respectively. A performance study of the device with a NFC potentiostat is shown in Figure 5. A composition and photograph of the NFC-operated 3D-ePAD are shown in Figure 5A-B. The linearity range of cholesterol detection was 1 to 500 μg/mL, and the LOD was 0.3 μg/mL. A comparison of the proposed paper-based device and other cholesterol sensors is given in Table 1. Among free-enzymatic cholesterol sensors, the limit of detection of the proposed method is inferior to that of some previous work. However, this proposed platform exhibits substantial advantages, as it is inexpensive (approximately 10.1 US$, with a division of 10 US$[22] for the reusable NFC potentiostat and 0.1 US$ for the 3D-ePAD), portable and disposable with a linear wide dynamic range of cholesterol quantification. The reproducibility was studied in terms of the relative standard deviation (RSD). NFC-operated 3D-ePAD was used for the detection of cholesterol at 10, 50, and 100 μM with different sensors. %RSD was found to be less than 4.25 (n = 7). Moreover, the device was enclosed in a sealed pouch with a desiccant and stored at 25 °C to examine its stability. After 90 days, the cholesterol detection current decreased to less than 80% compared with the initial reading. Hence, the device exhibits good stability for 90 days or approximately three months.

3.6. Specificity of Cholesterol Detection Using NFC-Operated 3D-ePAD

To further assess the selectivity of the proposed method, other commonly interfering compounds/ions in the human serum sample were evaluated including BSA, glucose, glycine, uric acid, ascorbic acid, NaCl, KCl, $MgCl_2$, and carbohydrates. The influence of interfering species was first examined individually at 100 μM on the analytical signal of 100 μM cholesterol. The current change ($\Delta I = I_{\text{tested species}} - I_{\text{blank}}$) between the test species and control after incubation is illustrated in Figure S4.

https://doi.org/10.1021/acsmeasuresciau.4c00012
ACS Meas. Sci. Au 2024, 4, 432−441

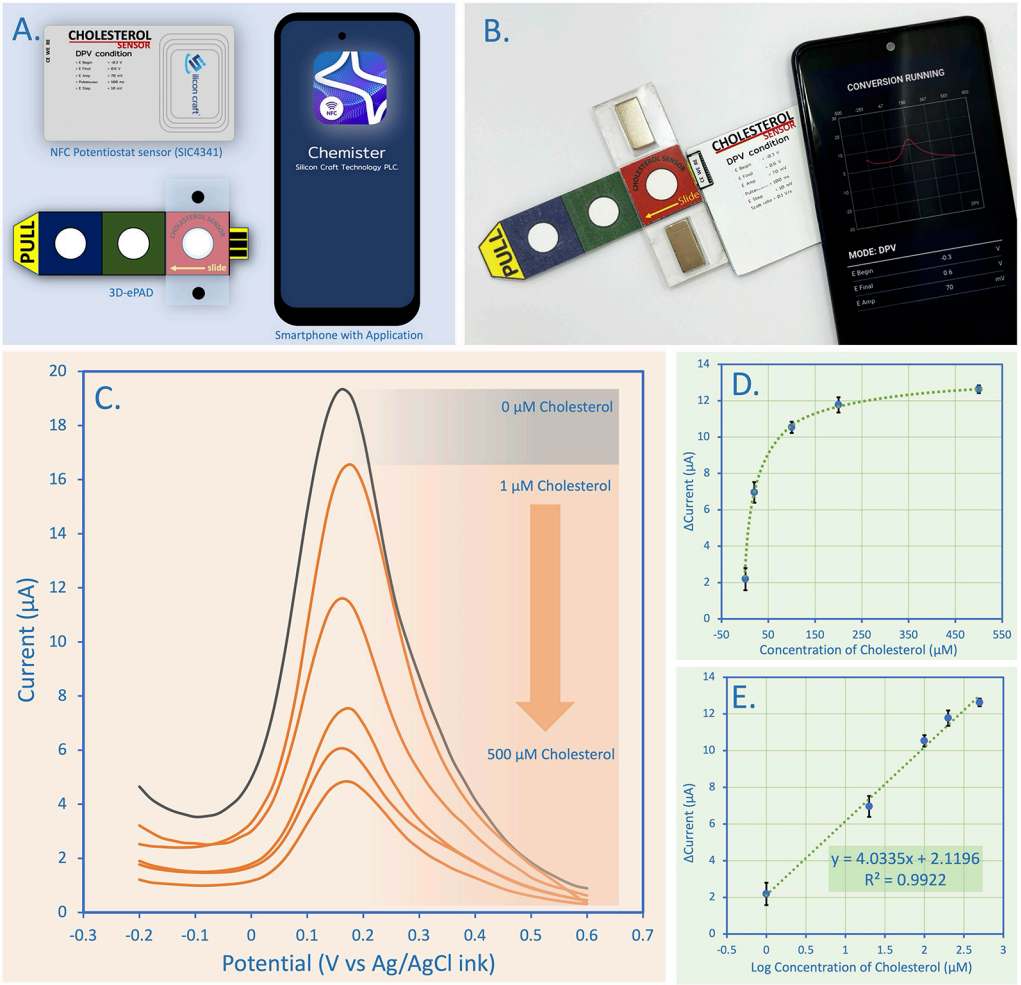

Figure 5. A composition (A) and photograph (B) of NFC-operated 3D-ePAD. (C) DPV responses of the NFC-operated 3D-ePAD sensor for detection of cholesterol at various concentrations. (D) The plot of the Δcurrent vs cholesterol concentration, (E) the linear relationship between Δcurrent and the logarithm of cholesterol concentration.

Negligible effects of signaling changes were found in the nonspecific compounds. In addition, only cholesterol was found to significantly increase the current change on 3D-ePAD. Moreover, the current signal of the interfering compound mixed solution containing 100 μM cholesterol was not significantly different from that of the cholesterol solution. The high specificity was established through the selective binding size between the interior cavity of β-CD and the cholesterol molecule. In addition, nonselective binding compounds/ions were washed into the waste chamber before analysis. These results indicate that no significant interference from these common interfering compounds in human serum occurred with the proposed platform. Therefore, the results indicated that 3D-ePAD can be applied in real serum sample applications with high specificity.

3.7. NFC-Operated 3D-ePAD Application in Real Human Serum

The analytical reliability and potential applicability of the 3D-ePAD were investigated by comparing results obtained with five human serum samples to those of a commercial cholesterol meter, namely, EasyTouch GCHb. The experimental findings are succinctly summarized in Table 2. The recoveries of cholesterol levels were detected within a 99−104% range, with relative standard deviations (RSDs) measuring less than 3.8% (n = 3). Furthermore, a paired test was conducted at a 95% confidence level, which yielded no notable disparities. The calculated t value of 2.29 was significantly lower than the critical t value of 2.77, with 4 degrees of freedom. Based on these findings, it can be concluded that 3D-ePAD is a reliable and feasible method for the accurate and precise detection of cholesterol levels in human serum.

4. CONCLUSION

In summary, we demonstrated a novel platform 3D-ePAD device combined with an NFC potentiostat sensor to detect cholesterol using β-CD modified on cellulose filter paper for the first time. The 3D-ePAD could eliminate undesirable procedures that involve multiple steps, as the immobilization of the target analyte, washing, and analysis step are combined into a single assay. The sensor system exhibited good sensitivity over a wide linear range from 1 to 500 μM with a detection limit of 300 nM. Furthermore, the developed 3D-ePAD sensor was applied by using an antibody- or enzyme-free system for biorecognition. In addition, 3D-ePAD could exhibit a high performance in terms of selectivity in the presence of interfering species to detect cholesterol efficiently in the nanomolar range. Thus, an NFC-operated 3D-ePAD sensor based on β-CD with unique features is the best alternative to

https://doi.org/10.1021/acsmeasuresciau.4c00012
ACS Meas. Sci. Au 2024, 4, 432−441

Table 1. Comparison with the Previous Nonenzymatic Approach for Cholesterol Quantification[a]

Sensing system	Substrate material	Electrochemical workstation			Linear range	LOD	ref
		Large	Medium	Small			
Pt NP/macroporous Au	Au	√			Up to 5 mM	0.15 mM	11
Ag NP/chitosan/GCE	GCE	√			0.02−3.3 mM	0.18 mM	12
Pt NP/CNT/ITO	ITO	√			0.005−10 mM	2.8 μM	13
MWCNT@MIP/CCE	CCE	√			10−300 nM	1 nM	37
Pt NP	Pt	√			2−8 mM	-	38
CNTs functionalized	SPE		√		1−50 μM	17 nM	39
Cu_2S NRS	Copper rod	√			0.01−6.8 mM	0.1 μM	40
L-MMT	ITO	√			1−20 mM	-	41
β-CD/PNAANI/rGO	GCE	√			1−50 μM	0.5 μM	17
β-CD@rGO	Pt wire	√			0.001−0.1 mM	1 μM	15
H+ modified L-MMT	ITO	√			1 mM	1 nM	42
β-CD@N-GQD/FC	GCE	√			0.5−100 μM	80 nM	43
Cu_2O NPs/TNTs	TNTs	√			24.4−622 mM	0.05 mM	44
β-CD/Fe_3O_4	SPE		√		2.88−150 μM	2.88 μM	16
MIP-MWCNTs/Au NPs	SPE	√			0.01−8 μM	0.01 μM	45
Au@NiO/PPy-GCE	GCE	√			0.01−0.1 mM	0.58 μM	46
β-CD on PAD	3D-ePAD	√			0.1−1000 μM	30 nM	this work
				√	1−500 μM	0.3 μM	

[a]Pt NP-platinum nanoparticles, Ag NP-silver nanoparticles, SPE-screen printed electrode, ITO-indium−tin-oxide, GCE-glassy carbon electrode, CPE-carbon paste electrode, MWNT-multiwall carbon nanotubes, L-MMT-Laponite-Montmorillonite, MIP-molecularly imprinted polymer, CCE-ceramic carbon electrode, Au NPs- gold nanoparticles, C_2O NPs-copper oxide nanoparticles, TNTs-titanium oxide nanotubes, Cu_2S NRS-copper(I)Sulfide nanoplates, β-CD-β-cyclodextrin, PNAANI- poly(*N*-acetylaniline), rGO-reduced graphene oxide, N-GQD-nitrogen-doped graphene quantum dots, Fc-ferrocene, PLE-pencil lead electrode, Au@NiO-gold nanoparticles@nickel(II) oxide, PPy- polypyrrole

Table 2. Summarized Results for the Detection of Cholesterol in Human Serum Samples Using NFC-Operated 3D-ePAD Platform and a Commercial Cholesterol Meter (n = 3)

Samples	Cholesterol Concentration (mg/dL) ± SD		% Recovery	% RSD
	By a commercial meter	By 3D-ePAD		
Serum 1	184 ± 2.84	181 ± 4.01	101.66	2.21
Serum 2	150 ± 3.21	145 ± 5.51	103.45	3.80
Serum 3	175 ± 1.54	171 ± 5.48	102.34	3.20
Serum 4	219 ± 2.94	221 ± 4.85	99.10	2.19
Serum 5	201 ± 3.54	195 ± 5.81	103.08	2.98

cholesterol nonenzymatic sensors due to its low cost, easy fabrication, and robustness. Notably, the sensor can be used as a prototype and further developed into a portable tool to diagnose other diseases. This platform can be applied for home to professional use.

■ ASSOCIATED CONTENT

Supporting Information

The Supporting Information is available free of charge at https://pubs.acs.org/doi/10.1021/acsmeasuresciau.4c00012.

Materials, reagents, and equipment; details of the composition and size of the oPAD and iPAD; the study of optimum conditions of cholesterol detection using 3D-ePAD consists of β-CD concentration and sample incubation time; DPV responses of the 3D-ePAD using commercial potentiostat for detection of cholesterol at various concentrations using the plot of the Δcurrent vs cholesterol concentration; the linear relationship between Δcurrent and the logarithm of cholesterol concentration; the Δcurrent obtained for studying various interfering substances using the 3D-ePAD biosensor; and the EIS qualitative results obtained from the different operation steps (PDF)

Video of the operation of the 3D-ePAD device (MP4)

■ AUTHOR INFORMATION

Corresponding Author

Sudkate Chaiyo − *The Institute of Biotechnology and Genetic Engineering and Center of Excellence for Food and Water Risk Analysis (FAWRA), Faculty of Veterinary Science, Chulalongkorn University, Bangkok 10330, Thailand;* orcid.org/0000-0002-4527-7041; Email: sudkate.c@chula.ac.th

Authors

Kanjana Kunpatee − *The Institute of Biotechnology and Genetic Engineering, Chulalongkorn University, Bangkok 10330, Thailand*

Kurt Kalcher − *Institute of Chemistry, Karl-Franzens University, Graz A-8010, Austria*

Abdulhadee Yakoh − *The Institute of Biotechnology and Genetic Engineering and Center of Excellence for Food and Water Risk Analysis (FAWRA), Faculty of Veterinary Science, Chulalongkorn University, Bangkok 10330, Thailand;* orcid.org/0000-0002-8392-5492

Kingkan Pungjunun − *Sensor Technologist, Silicon Craft Technology Public Company Limited, Bangkok 10900, Thailand*

Complete contact information is available at: https://pubs.acs.org/10.1021/acsmeasuresciau.4c00012

Author Contributions

Sudkate Chaiyo: Conceptualization, Writing - review and editing, Supervision, Project administration, Funding acquisition. **Kanjana Kunpatee**: Conceptualization, Methodology,

https://doi.org/10.1021/acsmeasuresciau.4c00012
ACS Meas. Sci. Au 2024, 4, 432−441

Formal analysis. **Abdulhadee Yakoh:** Formal analysis, Investigation. **Kurt Kalcher:** Supervision, Project administration. **Kingkan Pungjunun**: Resources, Investigation.

Notes

The authors declare no competing financial interest.

■ ACKNOWLEDGMENTS

This research was (partially) supported by the Asahi Glass Foundation, Japan (RES_63_313_61_003). Furthermore, this project is also funded by the National Research Council of Thailand and Chulalongkorn University: N42A650271. Finally, we would like to thank the ASEAN-European Academic University Network (ASEA-UNINET), the Austrian Federal Ministry of Education, Science, and Research, and the Austrian Agency for International Mobility and Cooperation in Education, Science, and Research (OeAD-GmbH) for financial support of mobility.

■ REFERENCES

(1) Ridker, P. M.; Danielson, E.; Fonseca, F. A.; Genest, J.; Gotto, A. M.; Kastelein, J. J.; Koenig, W.; Libby, P.; Lorenzatti, A. J.; MacFadyen, J. G.; et al. Reduction in C-reactive protein and LDL cholesterol and cardiovascular event rates after initiation of rosuvastatin: a prospective study of the JUPITER trial. *Lancet* **2009**, *373* (9670), 1175−1182.

(2) Huxley, R.; Lewington, S.; Clarke, R. Cholesterol, coronary heart disease and stroke: a review of published evidence from observational studies and randomized controlled trials. *Semin Vasc Med.* **2002**, *02* (3), 315−324.

(3) Igl, W.; Kamal-Eldin, A.; Johansson, A.; Liebisch, G.; Gnewuch, C.; Schmitz, G.; Gyllensten, U. Animal source food intake and association with blood cholesterol, glycerophospholipids and sphingolipids in a northern Swedish population. *Int. J. Circumpolar Health* **2013**, *72*, 21162.

(4) Kannel, W. B. Range of serum cholesterol values in the population developing coronary artery disease. *American journal of cardiology* **1995**, *76* (9), 69C−77C.

(5) Ma, H.; Shieh, K.-J. Cholesterol and human health. *Journal of American Science* **2006**, *2* (1), 46−50.

(6) Ying, Y.; Li, J.-X.; Chen, J.-c.; Jie, C.; Lu, X.-f.; Chen, S.-f.; Wu, X.-G.; Duan, X.-F.; Mo, X.-B.; Gu, D.-F. Effect of elevated total cholesterol level and hypertension on the risk of fatal cardiovascular disease: a cohort study of Chinese steelworkers. *Chinese medical journal* **2011**, *124* (22), 3702−3706.

(7) Solomon, A.; Kivipelto, M.; Wolozin, B.; Zhou, J.; Whitmer, R. A. Midlife serum cholesterol and increased risk of Alzheimer's and vascular dementia three decades later. *Dementia and geriatric cognitive disorders* **2009**, *28* (1), 75−80.

(8) Jeong, S. M.; Jang, W.; Shin, D. W. Association of statin use with Parkinson's disease: dose−response relationship. *Movement Disorders* **2019**, *34* (7), 1014−1021.

(9) Ahmadalinezhad, A.; Chen, A. High-performance electrochemical biosensor for the detection of total cholesterol. *Biosens. Bioelectron.* **2011**, *26* (11), 4508−4513.

(10) Kim, M. W.; Kim, Y. H.; Bal, J.; Stephanie, R.; Baek, S. H.; Lee, S. K.; Park, C. Y.; Park, T. J. Rational design of bienzyme nanoparticles-based total cholesterol electrochemical sensors and the construction of cholesterol oxidase expression system. *Sens Actuators B Chem.* **2021**, *349*, No. 130742.

(11) Lee, Y.-J.; Park, J.-Y. Nonenzymatic free-cholesterol detection via a modified highly sensitive macroporous gold electrode with platinum nanoparticles. *Biosens. Bioelectron.* **2010**, *26* (4), 1353−1358.

(12) Li, Y.; Bai, H.; Liu, Q.; Bao, J.; Han, M.; Dai, Z. A nonenzymatic cholesterol sensor constructed by using porous tubular silver nanoparticles. *Biosens. Bioelectron.* **2010**, *25* (10), 2356−2360.

(13) Yang, J.; Lee, H.; Cho, M.; Nam, J.; Lee, Y. Nonenzymatic cholesterol sensor based on spontaneous deposition of platinum nanoparticles on layer-by-layer assembled CNT thin film. *Sens. Actuators, B* **2012**, *171*−*172*, 374−379.

(14) Ali, M. A.; Solanki, P. R.; Patel, M. K.; Dhayani, H.; Agrawal, V. V.; John, R.; Malhotra, B. D. A highly efficient microfluidic nano biochip based on nanostructured nickel oxide. *Nanoscale* **2013**, *5* (7), 2883−2891.

(15) Agnihotri, N.; Chowdhury, A. D.; De, A. Non-enzymatic electrochemical detection of cholesterol using β-cyclodextrin functionalized graphene. *Biosens. Bioelectron.* **2015**, *63*, 212−217.

(16) Willyam, S. J.; Saepudin, E.; Ivandini, T. A. β-Cyclodextrin/Fe3O4 nanocomposites for an electrochemical non-enzymatic cholesterol sensor. *Analytical Methods* **2020**, *12* (27), 3454−3461.

(17) Yang, L.; Zhao, H.; Fan, S.; Zhao, G.; Ran, X.; Li, C.-P. Electrochemical detection of cholesterol based on competitive host−guest recognition using a β-cyclodextrin/poly(N-acetylaniline)/graphene-modified electrode. *RSC Adv.* **2015**, *5* (79), 64146−64155.

(18) Srisomwat, C.; Teengam, P.; Chuaypen, N.; Tangkijvanich, P.; Vilaivan, T.; Chailapakul, O. Pop-up paper electrochemical device for label-free hepatitis B virus DNA detection. *Sens Actuators B Chem.* **2020**, *316*, No. 128077.

(19) Punjiya, M.; Moon, C. H.; Matharu, Z.; Nejad, H. R.; Sonkusale, S. A three-dimensional electrochemical paper-based analytical device for low-cost diagnostics. *Analyst* **2018**, *143* (5), 1059−1064.

(20) Cheng, C.; Li, X.; Xu, G.; Lu, Y.; Low, S. S.; Liu, G.; Zhu, L.; Li, C.; Liu, Q. Battery-free, wireless, and flexible electrochemical patch for in situ analysis of sweat cortisol via near field communication. *Biosens. Bioelectron.* **2021**, *172*, No. 112782.

(21) Krorakai, K.; Klangphukhiew, S.; Kulchat, S.; Patramanon, R. Smartphone-based NFC potentiostat for wireless electrochemical sensing. *Applied Sciences* **2021**, *11* (1), 392.

(22) Pungjunun, K.; Yakoh, A.; Chaiyo, S.; Siangproh, W.; Praphairaksit, N.; Chailapakul, O. Smartphone-based electrochemical analysis integrated with NFC system for the voltammetric detection of heavy metals using a screen-printed graphene electrode. *Mikrochim. Acta* **2022**, *189* (5), 191.

(23) Barba, A. B.; Bianco, G. M.; Fiore, L.; Arduini, F.; Marrocco, G.; Occhiuzzi, C. Design and manufacture of flexible epidermal NFC device for electrochemical sensing of sweat. *2022 IEEE International Conference on Flexible and Printable Sensors and Systems (FLEPS)*, 2022; IEEE: pp 1−4.

(24) Xu, G.; Li, X.; Cheng, C.; Yang, J.; Liu, Z.; Shi, Z.; Zhu, L.; Lu, Y.; Low, S. S.; Liu, Q. Fully integrated battery-free and flexible electrochemical tag for on-demand wireless in situ monitoring of heavy metals. *Sens Actuators B Chem.* **2020**, *310*, No. 127809.

(25) Furusaki, E.; Ueno, Y.; Sakairi, N.; Nishi, N.; Tokura, S. Facile preparation and inclusion ability of a chitosan derivative bearing carboxymethyl-β-cyclodextrin. *Carbohydr. Polym.* **1996**, *29* (1), 29−34.

(26) Cheng, J. G.; Tian, B. R.; Huang, Q.; Ge, H. R.; Wang, Z. Z. Resveratrol functionalized carboxymethyl-β-cyclodextrin: synthesis, characterization, and photostability. *Journal of Chemistry* **2018**, *2018*, 6789076.

(27) Patil, N. V.; Netravali, A. N. Cyclodextrin-Based "Green" Wrinkle-Free Finishing of Cotton Fabrics. *Ind. Eng. Chem. Res.* **2019**, *58* (45), 20496−20504.

(28) Joseph, V.; Warhaftig, O.; Klein, S.; Levine, M. Paper-based manganese and β-cyclodextrin sensors for colorimetric sulfur dioxide detection. *Anal. Chim. Acta* **2022**, *1200*, No. 339629.

(29) Santhiago, M.; da Costa, P. G.; Pereira, M. P.; Correa, C. C.; de Morais, V. r. B.; Bufon, C. C. Versatile and robust integrated sensors to locally assess humidity changes in fully enclosed paper-based devices. *ACS Appl. Mater. Interfaces* **2018**, *10* (41), 35631−35638.

(30) Jiang, Q.; Chandar, Y. J.; Cao, S.; Kharasch, E. D.; Singamaneni, S.; Morrissey, J. J. Rapid, point-of-care, paper-based plasmonic biosensor for Zika virus diagnosis. *Advanced Biosystems* **2017**, *1* (9), No. 1700096.

https://doi.org/10.1021/acsmeasuresciau.4c00012
ACS Meas. Sci. Au 2024, 4, 432−441

(31) Chen, X.; Li, Y.; Yuan, X.; Li, N.; He, W.; Feng, Y.; Liu, J. Surface modification by β-cyclodextrin/polyquaternium-11 composite for enhanced biofilm formation in microbial fuel cells. *J. Power Sources* **2020**, *480*, No. 228789.
(32) Bint E Naser, S. F.; Liu, H.-Y.; Su, H.; Kouloumpis, A.; Carten, J. D.; Daniel, S. An Impedance-Based Approach for Sensing Cyclodextrin-Mediated Modulation of Membrane Cholesterol. *Langmuir* **2023**, *39* (28), 9831−9840.
(33) Aristovich, E. Non-invasive Measurement of Cholesterol in Human Blood by Impedance Technique: an Investigation by Finite Element Field Modelling. Ph.D. Thesis, City University: London, 2014.
(34) Qin, Q.; Bai, X.; Hua, Z. Electropolymerization of a conductive β-cyclodextrin polymer on reduced graphene oxide modified screen-printed electrode for simultaneous determination of ascorbic acid, dopamine and uric acid. *J. Electroanal. Chem.* **2016**, *782*, 50−58.
(35) Wang, H.; Zhou, Y.; Guo, Y.; Liu, W.; Dong, C.; Wu, Y.; Li, S.; Shuang, S. β-Cyclodextrin/Fe3O4 hybrid magnetic nano-composite modified glassy carbon electrode for tryptophan sensing. *Sens Actuators B Chem.* **2012**, *163* (1), 171−178.
(36) Chen, X.; Li, N.; Rong, Y.; Hou, Y.; Huang, Y.; Liang, W. β-Cyclodextrin functionalized 3D reduced graphene oxide composite-based electrochemical sensor for the sensitive detection of dopamine. *RSC Adv.* **2021**, *11* (45), 28052−28060.
(37) Tong, Y.; Li, H.; Guan, H.; Zhao, J.; Majeed, S.; Anjum, S.; Liang, F.; Xu, G. Electrochemical cholesterol sensor based on carbon nanotube@molecularly imprinted polymer modified ceramic carbon electrode. *Biosens. Bioelectron.* **2013**, *47*, 553−558.
(38) Yoon, H. S.; Lee, S. J.; Park, J. Y.; Paik, S. J.; Allen, M. G. A non-enzymatic micro-needle patch sensor for freecholesterol continuous monitoring. *SENSORS, 2014*; IEEE, 2−5 Nov. 2014, 2014; pp 347−350. DOI: 10.1109/ICSENS.2014.6985005.
(39) Saha, M.; Das, S. Fabrication of a nonenzymatic cholesterol biosensor using carbon nanotubes from coconut oil. *Journal of Nanostructure in Chemistry* **2014**, *4* (1), 94.
(40) Ji, R.; Wang, L.; Wang, G.; Zhang, X. Synthesize Thickness Copper (I) Sulfide nanoplates on Copper Rod and It's Application as Nonenzymatic Cholesterol Sensor. *Electrochim. Acta* **2014**, *130*, 239−244.
(41) Joshi, N.; Rawat, K.; Solanki, P. R.; Bohidar, H. B. Enzyme-free and biocompatible nanocomposite based cholesterol sensor. *Biochemical Engineering Journal* **2015**, *102*, 69−73.
(42) Joshi, N.; Sharma, A.; Asokan, K.; Rawat, K.; Kanjilal, D. Effect of hydrogen ion implantation on cholesterol sensing using enzyme-free LAPONITE®-montmorillonite electrodes. *RSC Adv.* **2016**, *6* (27), 22664−22672.
(43) Ganganboina, A. B.; Doong, R.-a. Functionalized N-doped graphene quantum dots for electrochemical determination of cholesterol through host-guest inclusion. *Microchimica Acta* **2018**, *185* (11), 526.
(44) Khaliq, N.; Rasheed, M. A.; Cha, G.; Khan, M.; Karim, S.; Schmuki, P.; Ali, G. Development of non-enzymatic cholesterol biosensor based on TiO2 nanotubes decorated with Cu2O nanoparticles. *Sens. Actuators, B* **2020**, *302*, No. 127200.
(45) Jalalvand, A. R. Fabrication of a novel molecularly imprinted biosensor assisted by multi-way calibration for simultaneous determination of cholesterol and cholestanol in serum samples. *Chemometrics and Intelligent Laboratory Systems* **2022**, *226*, No. 104587.
(46) Nagarajan, A.; Sethuraman, V.; Sridhar, T. M.; Sasikumar, R. Development of Au@NiO decorated polypyrrole composite for non-Enzymatic electrochemical sensing of cholesterol. *Journal of Industrial and Engineering Chemistry* **2023**, *120*, 460−466.

https://doi.org/10.1021/acsmeasuresciau.4c00012
ACS Meas. Sci. Au 2024, 4, 432−441